Target Chamber Design Considerations for the APEX Light Ion Beam Fusion Facility

R.R. Peterson, R.L. Engelstad, G.A. Moses, E.G. Lovell

May 1987

UWFDM-724

FUSION TECHNOLOGY INSTITUTE

UNIVERSITY OF WISCONSIN

MADISON WISCONSIN

Target Chamber Design Considerations for the APEX Light Ion Beam Fusion Facility

R.R. Peterson, R.L. Engelstad, G.A. Moses, E.G. Lovell

Fusion Technology Institute
University of Wisconsin
1500 Engineering Drive
Madison, WI 53706

http://fti.neep.wisc.edu

May 1987

UWFDM-724

TARGET CHAMBER DESIGN CONSIDERATIONS FOR THE APEX LIGHT ION BEAM FUSION FACILITY

Robert R. Peterson

Roxanne L. Engelstad

Gregory A. Moses

Edward G. Lovell

Fusion Technology Institute
1500 Johnson Drive
University of Wisconsin-Madison
Madison, Wisconsin 53706

May 1987

UWFDM-724

ABSTRACT

The PBFA-II facility could be modified in the early 1990's to provide an ion beam powerful enough to drive a 100 MJ ICF target to ignition and burn. The modified facility, called APEX, would include the construction of a target chamber which would contain the target explosion. We have analyzed the target chamber gas behavior and structural response and have chosen a 50 cm radius target chamber as the base case design. We have also studied designs other than the base case and discuss the design options.

I. INTRODUCTION

There exists the possibility of modifying the PBFA-II pulsed power ion accelerator to give it the ability to implode a high yield (100 MJ) Inertial Confinement Fusion (ICF) target to ignition. This could occur in the early 1990's. The modification would involve changing the pulsed power components near the center of the device and directing the ion beam into the basement of the existing PBFA-II building. Proper voltage ramping and bunching in a plasma channel would provide a pulse shaped ion beam at the target. In the basement, the ion beam would enter a target chamber where the target explosions would take place. Scientists at Sandia National Laboratory, the Naval Research Laboratory, TRW and the University of Wisconsin have been studying the feasibility of this plan, called APEX.

A single 100 MJ target explosion will release enough neutrons to activate the target chamber, whether it is made of steel or aluminum. The chamber will remain too radioactive to handle for up to a month, which makes work on the target chamber very difficult. We have proposed a target chamber that is small enough to be remotely removed after each target explosion. The analysis of such a target chamber is the topic of this paper.

II. TARGET CHAMBER ANALYSIS

II.A. Introduction

The target chamber of APEX is required to contain the target explosion and resultant radioactive debris. An unusual feature of this target chamber is that it is removed after a single shot so that the major source of induced radiation in the experimental facility is eliminated. For this reason, smaller chambers are operationally preferable. Smaller sizes are possible only if vaporization of the inside wall of the target chamber is acceptable. Vaporization and subsequent recondensation of wall material complicate the analysis of the target chamber design [II-1]. Structural requirements, on the other hand, are less complicated because fatigue effects are not an issue.

In this chapter, we will first discuss some of the physics issues that are relevant to such a target chamber. We will then describe our approach towards analyzing the target chamber design. We will then present results of this analysis and conclude with some recommendations.

II.B. Physics Issues

Radioactivity induced in the APEX target chamber following a single 100 MJ target shot is a severe problem. A proposed solution is to make the target chamber as small as possible, so that it may be removed after each successful target explosion. The minimum target chamber radius is determined by the strength of the target chamber structure against rupture on a single shot. The radius determined by this criterion is small enough that the surface of the target chamber is vaporized. This complication has a great impact on the behavior of the target chamber gas and the pressure loading on the chamber wall.

The pressure loading on the chamber wall may be thought of as stemming from three sources: the static pressure of the vaporized wall material that fills the target chamber, the impulse due to shocks in the gas that are caused by the target explosion, and the recoil impulse from the vaporization of wall material. The vaporization of matter and the formation and propagation of shocks in the target chamber gas are effects that interact with each other in such a way that they must be studied in a consistent manner. First wall vaporization is due to the volumetric deposition of target generated x-rays, the surface deposition of target debris ions and the surface deposition of thermal radiation from the chamber gas. This vaporization is complicated because the surface layer of the first wall material receives more energy than required for vaporization, while the sublayers receive less energy than that required for heating to the sublimation temperature, and some have energy densities in between. It is unclear what happens to material in this third situation.

The transport of x-rays, ions, and thermal radiation onto the first wall depends on the density and temperature of the chamber gas. The condition of the chamber gas is complicated as the shock wave of vaporized material rushing off of the walls of the target chamber collides with the shock wave that is directly generated in the chamber gas by the target explosion. This gas collision and intermixing may insulate the chamber wall from the direct effects of the target generated blast, though the vaporized mass from the first wall may recoil off of the target generated blast wave and find its way back to the wall in the form of a shock wave.

The vaporization and recondensation of material in ICF target chambers can be broken down into two distinct phases [II-2,II-3,II-4]: 1) rapid adiabatic vaporization that is due to essentially instantaneous absorption of target generated x-rays and 2) slow vaporization due to energy that is radiated from the target chamber gas over a long enough time that vaporization is limited by heat transfer into the bulk of the first wall. If the target chamber is initially filled with a low density gas, the x-rays from the target deposit mostly in the target chamber wall (phase 1 is dominant), whereas in schemes with higher gas densities this energy is mainly absorbed in the gas (phase 2 will dominate).

In the case of low chamber gas density, both superheated vapor and vapor at the local boiling temperature of the vaporizing material come off of the surface in a complex way. In the chamber, this vapor will meet with energetic target debris ions and will be further heated. Radiation from this heated vapor will cause additional first wall vaporization and drive hydrodynamic forces which will move the vapor throughout the chamber. Eventually, condensation takes place back onto the chamber wall due to heat losses to the wall and through the wall by conduction. In this case, the presence of noncondensible gases may or may not affect the rate of condensation.

In the high density gas case, the x-ray and debris energy from the target create a fireball in the target chamber gas. Some of the x-ray energy reaches the wall and vaporizes wall material. The radiant energy from the fireball at the first surface is spread out over a long enough time that heat conduction into the material can reduce the amount of vaporization. The vaporized material mixes with the noncondensible target chamber gases, where it is moved about the target chamber by the hydrodynamic motion of the fireball. The rate of condensation can be greatly reduced by the presence of the noncondensible gases.

For small chambers with high vaporization levels, the vaporized mass is generally much larger than the initial mass of noncondensible cavity gas. Therefore, the static part of the wall pressure is mostly due to the vaporized mass. If the vaporized mass is treated as an ideal gas, one can write the static pressure as,

$$p^{static} = 2E/3V, \quad (1)$$

where E is the energy in the vapor and V is the volume of the target chamber. One should note that the mass of the vapor does not enter into Eq. (1). This is because the number density is proportional to and the energy density is inversely proportional to the vaporized mass. This assumes that the energy E is not dependent on the vaporized mass. When trying to estimate the static part of the pressure we have conservatively assumed that E is the total non-neutronic energy from the target (neglecting losses into the first wall).

A separate issue of vaporization is the eventual condensation site. This is important because the vapor will be at least somewhat radioactive and because the deposition of vaporized material could damage items in APEX that would otherwise survive. The material that is vaporized will condense over time onto surfaces and nucleation sites in the target chamber. The physics of this process is very complicated and difficult to simulate. Complications arise because the sticking coefficient, the fraction of atoms sticking to a surface, can vary greatly depending on the species of the condensing atoms or molecules and the condensing surface [II-5]. Also, the process by which vapor atoms begin condensing on nucleation sites in the gas itself is very difficult to predict without experimentation.

II.C. Methods of Analysis

We chose a set of target emanations that is consistent with light ion beam fusion targets. We then used the CONRAD computer code to simulate the vaporization of material from the chamber walls, the behavior of the resulting mixture of original gas and vaporized material, and the condensation of the vaporized material. One of the results of the CONRAD code is the pressure on the wall as a function of time. This is then used to calculate the mechanically induced stresses in the target chamber walls.

II.C.1. Target Emanations

The x-ray and ion spectra and energy partitioning that result from the target explosion are required for analysis of the target chamber behavior. We do not know yet what the targets used in APEX will look like, so we have chosen the target designed by Bangerter et al. [II-6], as one that is typical for light ion beam driven fusion. This target design was slightly modified into the form shown in Fig. 1. There the target is shown in its initial form and in its configuration at the start of its burn. The burning of the target was simulated with the PHD-IV computer code [II-7]. This simulation provides the time-dependent spectrum of x-rays leaving the target and the debris ion energies. These results have been reported elsewhere [II-8,II-9] and are also shown in Fig. 2 and Table 1. The target yield in these results is normalized to 100 MJ. The x-ray spectrum shown is integrated to 3.5 ns, where the hard component is due to x-rays from the burning fuel, while the soft are from the whole target. We believe that the 2.8 MJ in debris is lower than one would actually measure leaving a typical target because the conversion of neutrons into thermal energy in the compressed fuel capsule has been neglected. This may raise the debris energy to 5 or 6 MJ.

In calculating the target emanations, we have assumed that the targets are spherical and that they are of a particular spherical design. In fact, the targets will probably not be of this design and they may not be spherical. A different spherical design may change the x-ray and ion spectra and the partitioning of the target yield. A non-spherical target may release its

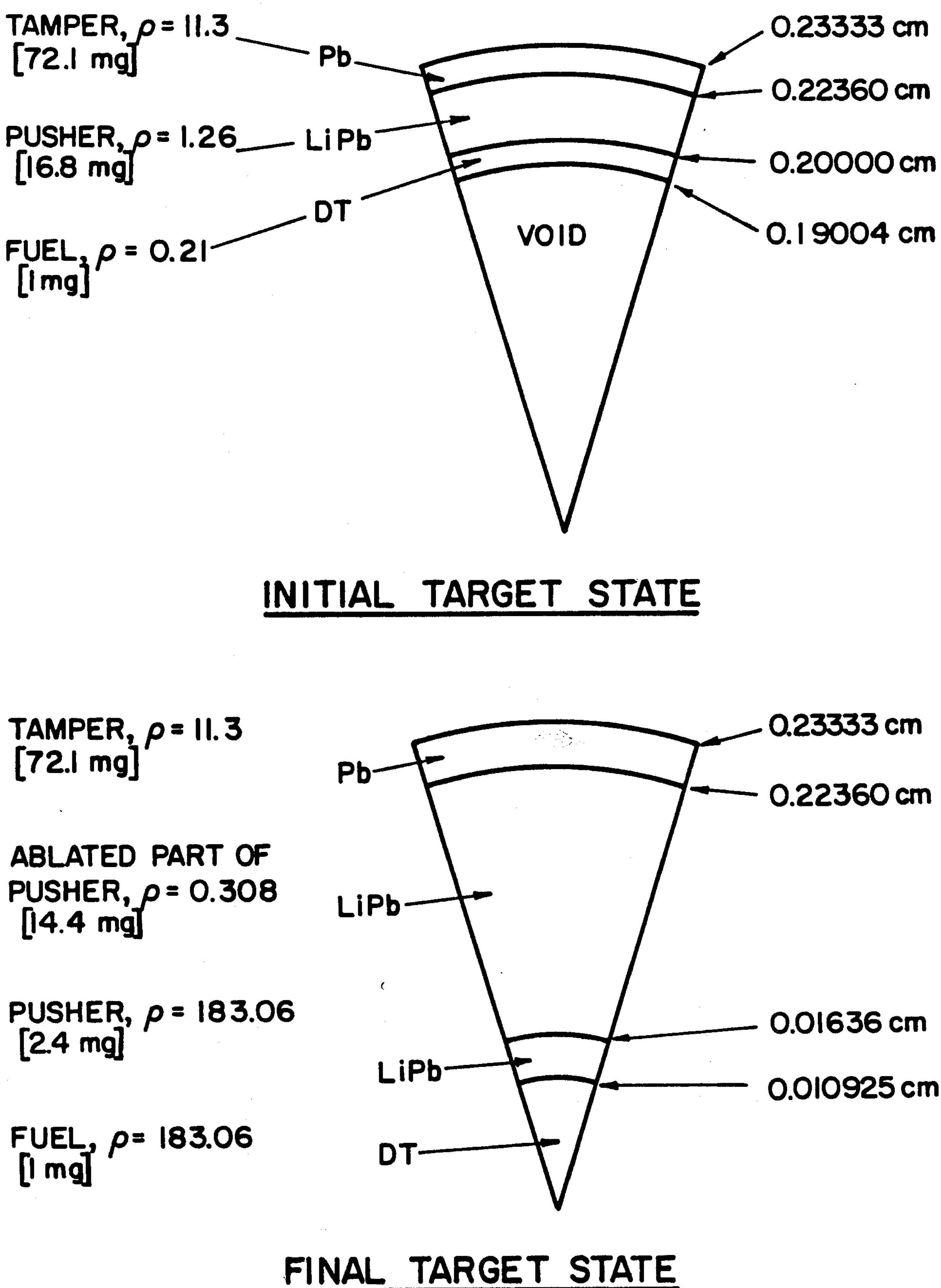

Fig. 1. Light Ion Fusion Target.

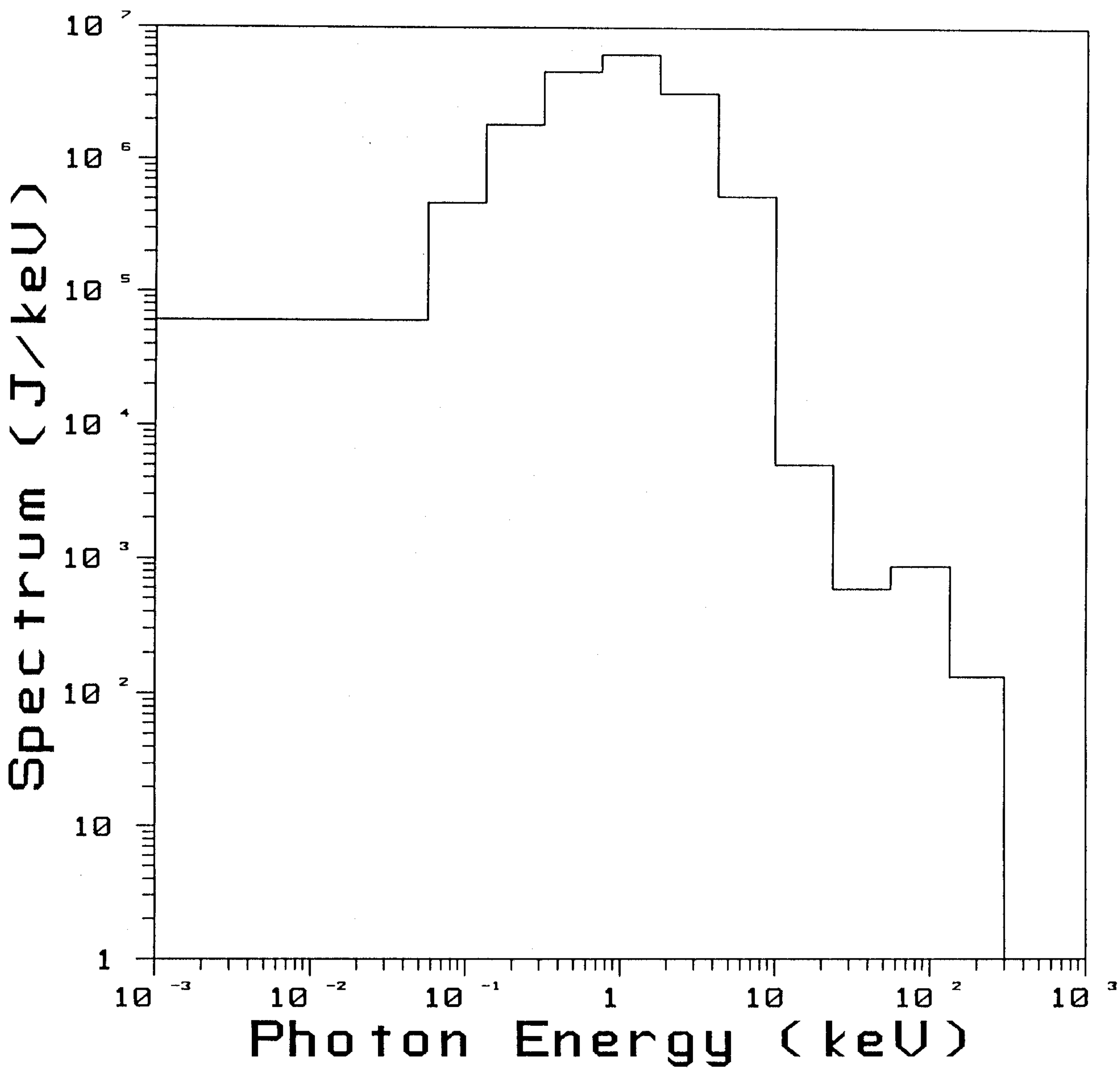

Fig. 2. Target X-ray Spectrum for HIBALL Type Target.

Table 1. Target Yield Energy Partition and Ion Energies

Energy Partition	
Fusion Yield	95.2 MJ
Neutron Yield	71 MJ
X-ray Yield	20 MJ
Debris Ion Yield	2.6 MJ
Endoergic Neutron Reactions	1.6 MJ
Debris Ion Energies	
Debris Ion Yield	2.6 MJ
Average Energy per Nucleon	0.85 keV/amu
Deuterium	1.70 keV
Tritium	2.55 keV
Helium	3.40 keV
Lithium	5.90 keV
Lead	176 keV

energy along preferred directions and could have spectra that vary with direction. These affect the details of how the first wall of the target chamber and other material vaporizes or otherwise responds to the target explosion. We have tried to design the target chamber in a conservative enough manner that these changes will not influence the survival of the target chamber.

II.C.2. Simulation of Chamber Gas Behavior

We have used the CONRAD [II-10] computer code to model the behavior of the target chamber gases. This Lagrangian hydrodynamics computer code models the deposition of x-rays and ions from a target into a target chamber gas and wall, vaporization of wall material, radiation transport and hydrodynamic motion in the gas, and final condensation of the vapor back onto the walls of the target chamber.

The CONRAD computer code attempts to model the behavior of a radiating, moving vapor and a material that is vaporizing or on which vapor is condensing by dividing the problem into two separate regions. The vapor, one of the regions, is modeled with Lagrangian hydrodynamics and multigroup radiative heat transfer. The unvaporized material, the other region, is modeled with a standard finite difference heat transfer method. From this point on, the term "material" will refer to the unvaporized material. Each of these sections is treated with rather standard numerical techniques. There is little experience in how to model the heat and mass transfer between the two regions. For this reason, there have been some options written into the code that allow the user to choose, for example, what model to use for rapid vaporization.

There has been considerable effort devoted to modeling the coupling between the target explosion and the gas and between the material and the gas. Multigroup x-ray deposition in the gas and surface material is calculated either as though it were instantaneous or in a time-dependent manner, or both ways. The energy from target debris ions is deposited in the gas as calculated by a modified form of Mehlhorn's model [II-11]. The time-of-flight of the ions is considered. The Lagrangian zones are dynamically rezoned as mass is transferred between the surface material and the vapor. Data tables of equations-of-state and opacities are read by CONRAD and are provided by the MIXERG computer code [II-12].

An effect that may seriously limit the condensation rate is that the equilibrium boiling temperature of the condensing material is a function of the local vapor density. Or, in a microscopic sense, the evaporation rate is a function of the surface temperature of the material, while the condensation rate is a function of the properties of the vapor near the wall; the net condensation rate is the difference between the two. The choice of these alternative approaches to the same effect is a option in CONRAD.

II.C.3. Reaction Chamber Mechanical Modeling

The shapes considered for the APEX target chamber are a compact capped cylinder and a spherical shell. The cylindrical vessel has practical advantages related to construction and operation but will generally be more highly stressed for a given dynamic pressure. The spherical shell is the optimum structure for sustaining the anticipated blast wave and has been the model used in this scoping study.

For the mechanical analysis, the motion is completely symmetric, i.e., the shell is always spherical and simply expands and contracts with the same radial displacement component everywhere on the sphere. The natural vibration frequency in this case depends upon the elastic modulus, density, Poisson's ratio, and the shell radius but is independent of the thickness. An impulsive pressure will develop dynamic stresses which are independent of radius and are essentially the same for 2-1/4 Cr-1 Mo steel and aluminum 6061 because of similar material property ratios. Representing the shock as an impulse has been shown to be satisfactory in the analysis of target chambers. However, for the smaller vessels, the initial spike is followed by a substantial quasi-static pressure. For an accurate assessment of such a history, a conventional Runge-Kutta integration routine was adapted to the problem. Numerical pressure data from the CONRAD blast wave simulation computer code was used directly with the shell equations of motion. Variable time step sizes were also used - finer for the rapidly varying pressure spike and more coarse for the relatively constant afterpressure. The program was benchmarked against similar classic analytical problems with available solutions and shown to be in excellent agreement.

II.D. Results of Analysis

We have calculated the response of the target chamber gas and structure to the target blast by using the methods outlined above. The calculations address five areas: a base case target chamber design, a parametric study of target chambers of different radii, the option of a chamber with no graphite liner, the propagation of shock waves down the beam propagation tube, and the condensation of vaporized material. We realize that there may be other topics of interest, but we have kept to this list of calculations to keep within the limited scope of this project.

II.D.1. Base Case

The base case target chamber design for APEX is presently a spherical vessel 50 cm in radius, with a 1 cm thick graphite liner on the inside surface of the vessel. Another option, which is discussed in a following section, is a vessel without such a liner. The structural wall of the vessel is made either of Al 6061 or 2-1/4 Cr-1 Mo steel. The base case design is shown in Fig. 3. The initial target chamber gas for the base case is 100 torr of He. The structural wall of the vessel is 5 cm thick for both materials.

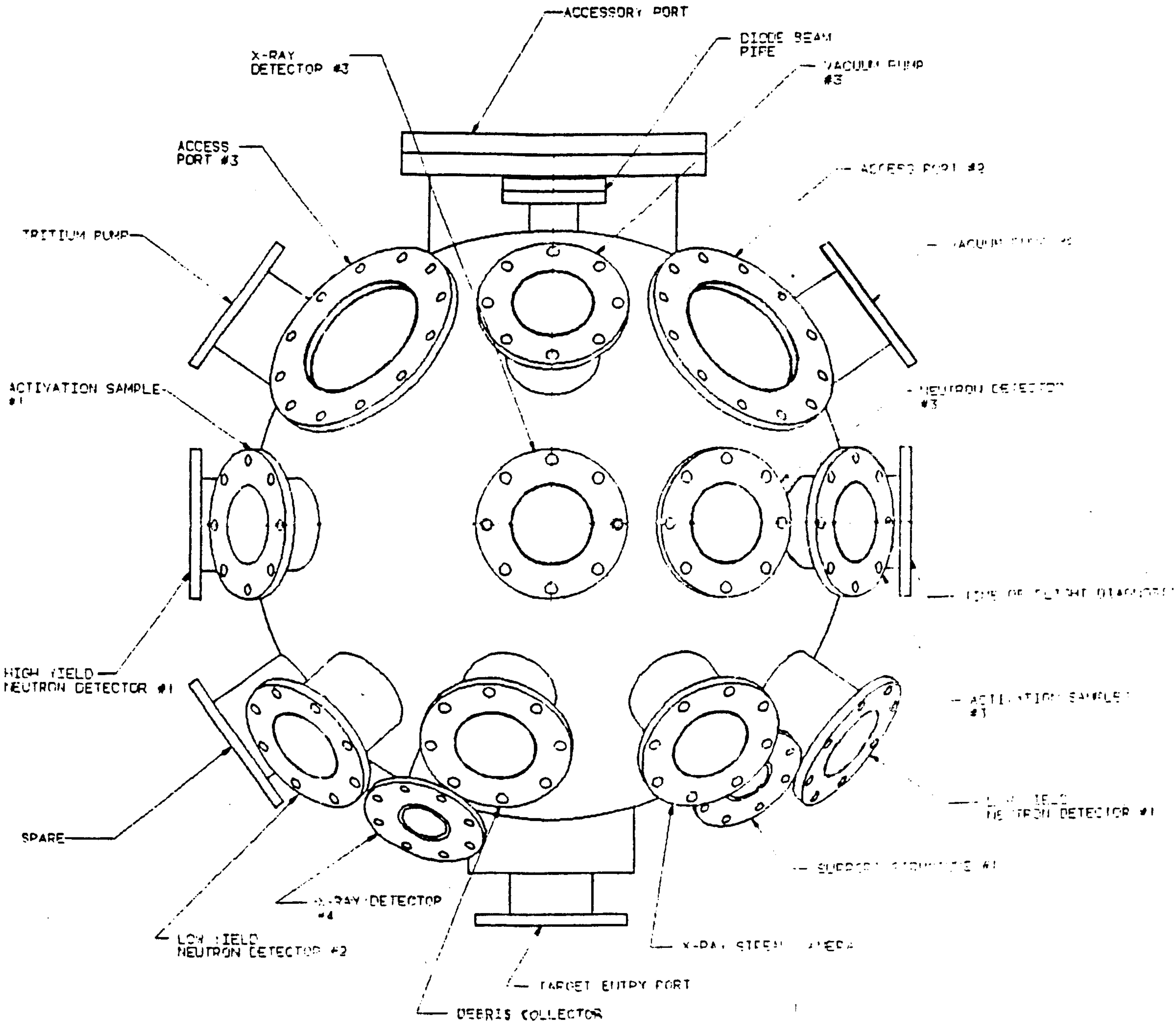

Fig. 3. Base Case Target Chamber Design for APEX.

We have used the target emanations given above and the CONRAD code to simulate the response of the target chamber gas and wall to the target explosion. The x-rays vaporize about 80 grams of graphite from the chamber wall, compared with 12 grams of initial gas mass. The effects of this added mass are clearly shown in the plot in Fig. 4, where the positions of the Lagrangian zone boundaries are plotted against time. One notices here that an early outward moving shock has been turned back by the mass coming off of the wall. One sees that both the vaporized mass and the original outward moving shock wave reflect off of each other and the reflected vaporized mass strikes the wall. A large shock is driven inward and is then reflected at the center of the cavity and again a shock reaches the wall. This one-dimensional simulation overestimates the reflection of the shock at the center of the chamber, so the strength of that shock when it reaches the wall is certainly less than that predicted by this code. The pressure on the wall, as predicted by the code, is shown in Fig. 5. Because we do not believe that the second shock striking the wall is very strong, we only show the pressure from the first shock. The static pressure, defined as

$$p^{static} = 1.602 \times 10^{-19} \, nT(1 + Z) \ , \tag{2}$$

where n, T, and Z are respectively the average number density in cm^{-3}, temperature in eV, and charge state in the gas, is 5.5 MPa.

In addition to the shock and static pressures, there is a load on the vessel wall due to the recoil impulse from vaporization. This is just equal to the momentum of the vaporized material as is moves off of the wall per unit

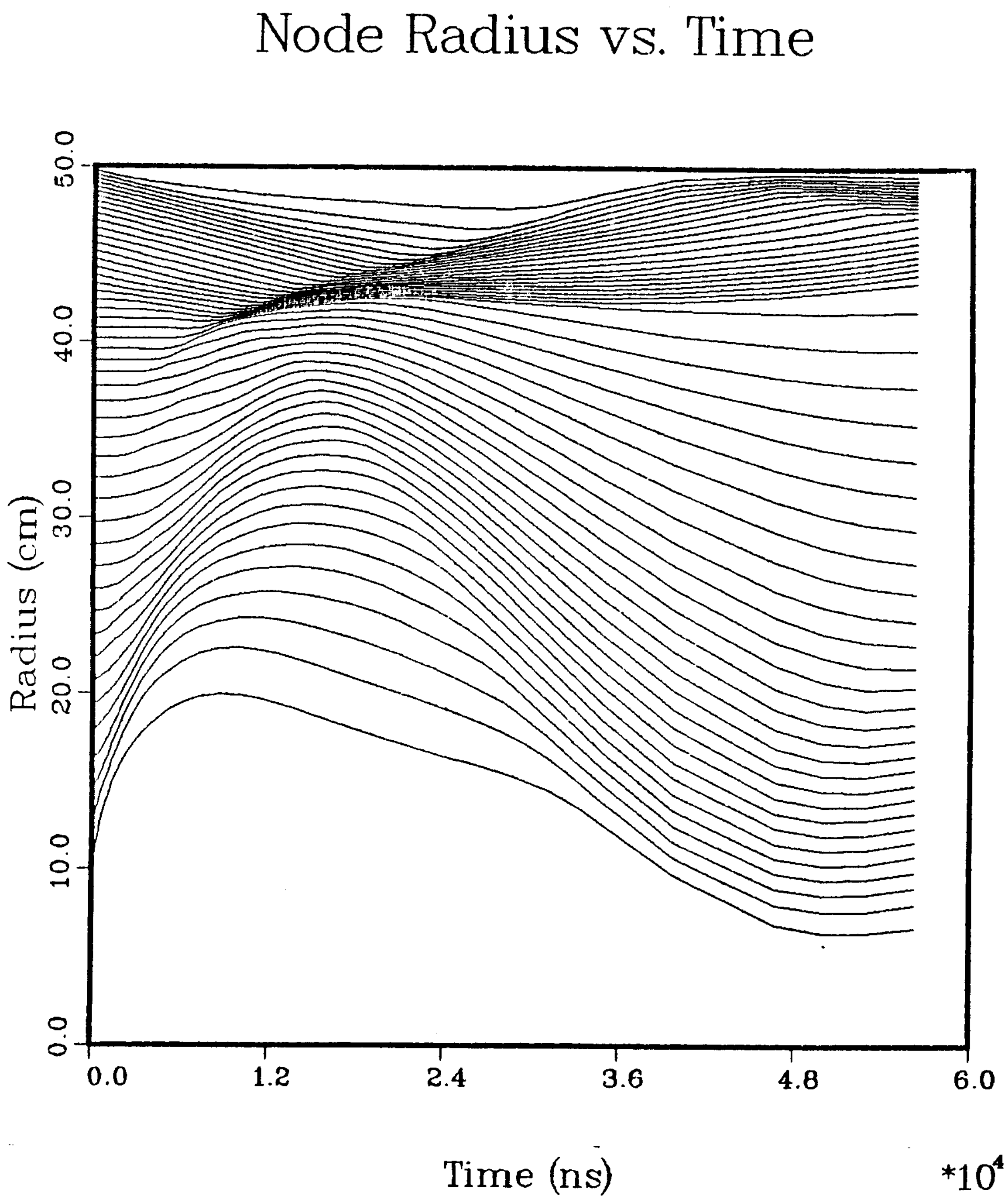

Fig. 4. Positions of Lagrangian Zone Boundaries versus Time for APEX Base Case.

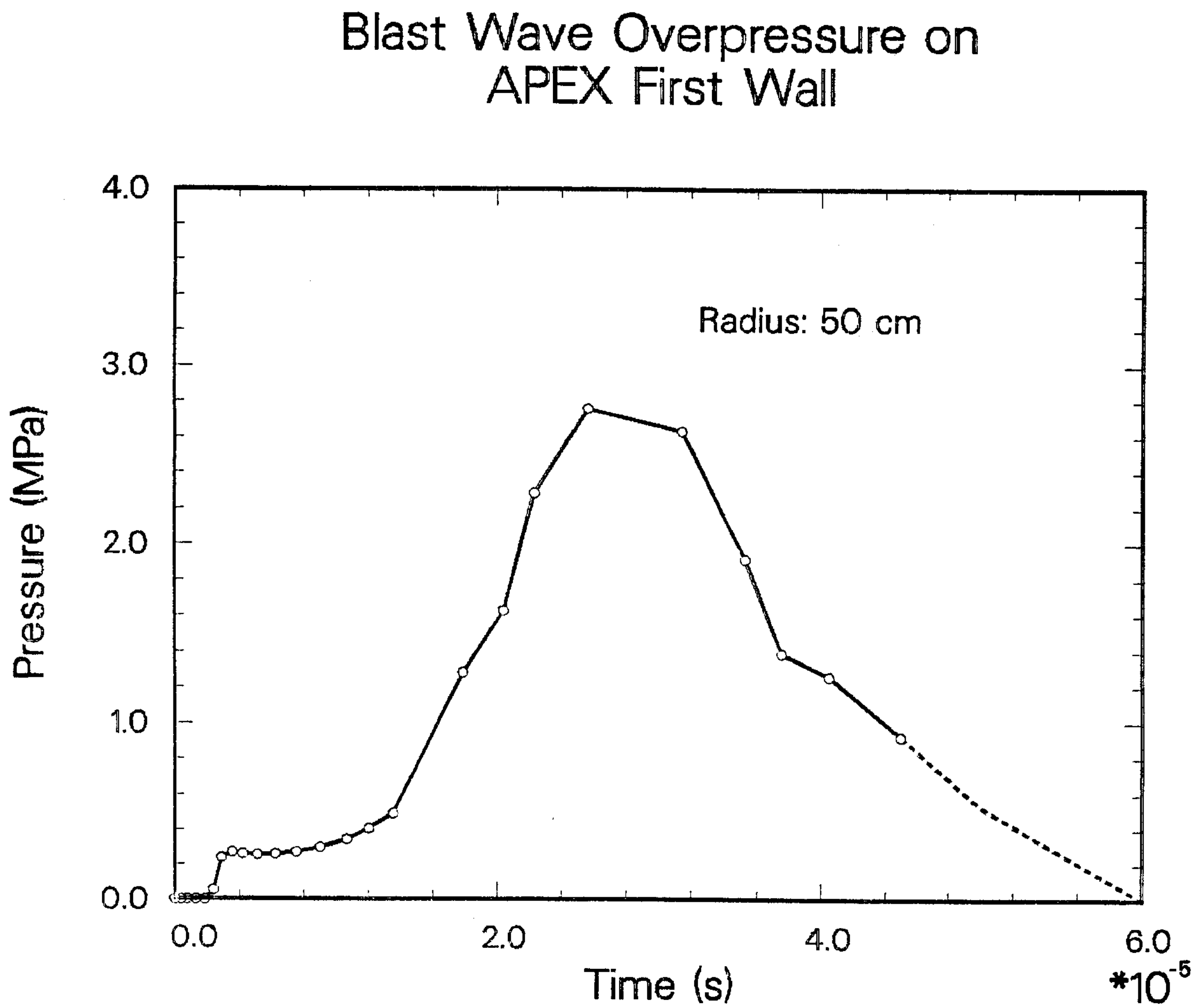

Fig. 5. Pressure on Target Chamber Wall versus Time for APEX Base Case.

of wall surface area. The base case has 76 grams of vaporized material that leaves the surface at roughly 2 km/s. The impulse is therefore 48 Pa-s. This constitutes a significant but not dominant portion of the loading on the wall.

The mechanical stresses induced in the target chamber walls by the pressures in Fig. 5 have been calculated in the method described above. We have calculated the wall stresses considering impulsive loadings from the pressure pulse in Fig. 5 and the recoil from the vaporization and the steady state loading from static pressure given in Eq. (2). The stress history is given in Fig. 6. These results are valid for both Al 6061 and 2-1/4 Cr-1 Mo steel, and for wall thicknesses of 1.25, 2.5 and 5.0 cm. We feel that these calculations are conservative. Even with this conservatism, the maximum stress for the 5.0 cm thick base case is only about 40 MPa, while the yield stress is 270 MPa for Al 6061 and is 255 MPa for steel. Therefore, the mechanical stresses are always a small fraction of the yield stress and the target chamber should easily survive a single shot.

II.D.2. Parametric Study

We have studied target chamber designs other than the base case. Our purpose in this is to discover the flexibility allowed in the design of the APEX target chamber. One way of studying this is to vary the target chamber radius. Since external constraints may dictate limits on the radius, we should study the possibility of changing the radius.

We have simulated the behavior of the target chamber gas for an initial gas of 100 torr of helium for target chamber radii from 35 cm to 100 cm. We have only studied the 50 cm radius base case in detail, so the results for the other radii must be classified as preliminary. The results are summarized in Table 2.

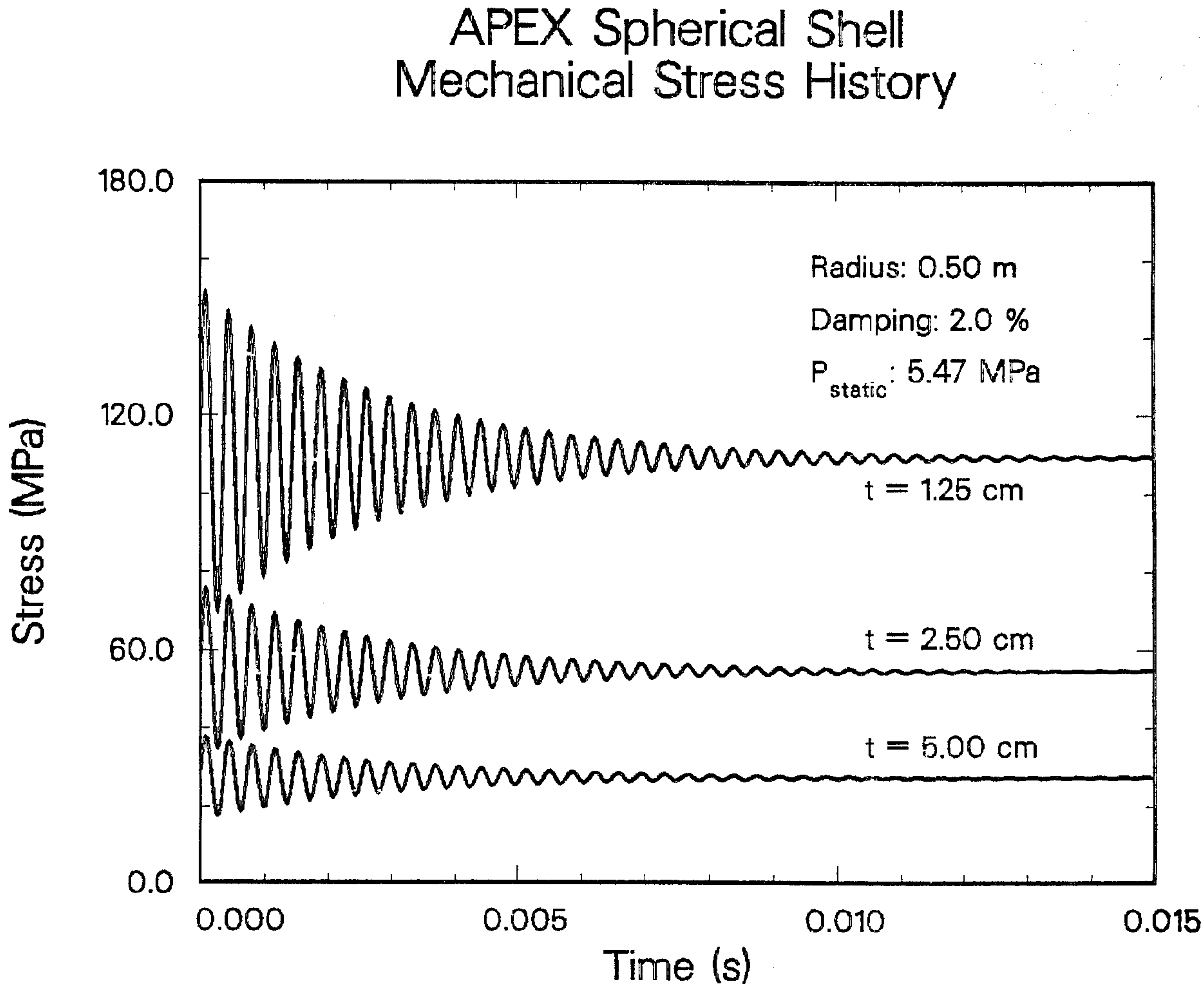

Fig. 6. Mechanical Stress History in Target Chamber for the APEX Base Case. P static is calculated as in Eq. (2). Wall thicknesses are 1.25, 2.5 and 5.0 cm.

Table 2. Parametric Study

Radius (cm)	100	50	45	40	35
Gas Energy (MJ)	10.4	11.6	11.4	11.0	10.6
Vaporized Mass (g)	24	76	85	92	96
Gas Mass (g)	123	88	94	98	100
Energy Density (MJ/g)	0.08	0.13	0.12	0.11	0.11
Ambient Gas Temp (eV)	2.0	2.1	2.1	2.0	2.0
Charge State (esu)	0.13	0.91	0.87	0.83	0.79
Average Density ($10^{18}/cm^3$)	4.4	8.4	12	18	28
Blowoff Velocity (km/s)	2	2	2	2	2
Static Pressure (MPa)	1.6	5.5	7.7	11	16
Recoil Impulse (Pa-s)	4	48	67	92	125
Blast Impulse (Pa-s)	120	75	24	7	0

Acknowledging the preliminary nature of some of the results, we still can comment on some tendencies that we have observed while varying the target chamber radius. As one reduces the radius, vaporization becomes the dominant phenomenon. At a radius of 100 cm, target x-rays vaporize 24 grams of wall material, while there is initially 99 grams of gas in the chamber. This low amount of vaporization means that the shielding of the wall from the blast wave by vaporized material is not particularly effective and that the recoil impulse is only 4 Pa-s compared with the blast wave impulse of 120 Pa-s. As one decreases the radius, the vaporization increases and so does the effectiveness of the vapor shielding and the recoil impulse. At a radius of 35 cm, 96 grams of wall material vaporizes compared with 4 grams initially in the cavity gas. The recoil impulse is 125 Pa-s, while the impulse of the blast wave on the wall is zero, meaning the vapor shielding is totally effective. Because the average total gas density increases as the radius decreases, the static pressure defined in Eq. (2) increases from 1.6 MPa to 16 MPa as the radius decreases from 100 cm to 35 cm.

Because we need to further study some of the results in Table 2 to verify their accuracy, we have done structural analysis for the 100 cm and 50 cm radius cases only. The blast wave pressure pulse and the static pressure for the 100 cm radius case is shown in Fig. 7. The recoil impulse is not important for a 100 cm radius and is not included. We have calculated the mechanical stress histories in walls 1.25, 2.5, and 5 cm thick and have plotted them in Fig. 8. The stresses for all cases are less than one half of the yield stress for steel and aluminum. For a 5 cm thick wall, the same as in the base case, the maximum stress is about 35 MPa, while it is 40 MPa for the 50 cm radius base case.

We have done a preliminary investigation of the situation when the cavity gas is initially 0.1 torr of helium. This low density may be required by the diagnostics or there may be chamber design advantages. We have found two differences between the 100 torr and the 0.1 torr cases: the low density case will experience somewhat more vaporization, and with a low initial density the debris ions deposit in the vaporized matter, while with 100 torr of helium they deposit in the background gas. For a 50 cm radius chamber, 150 grams of carbon are vaporized from the wall with the low density, while 75 grams are vaporized in the base case with 100 torr. We have tested the importance of

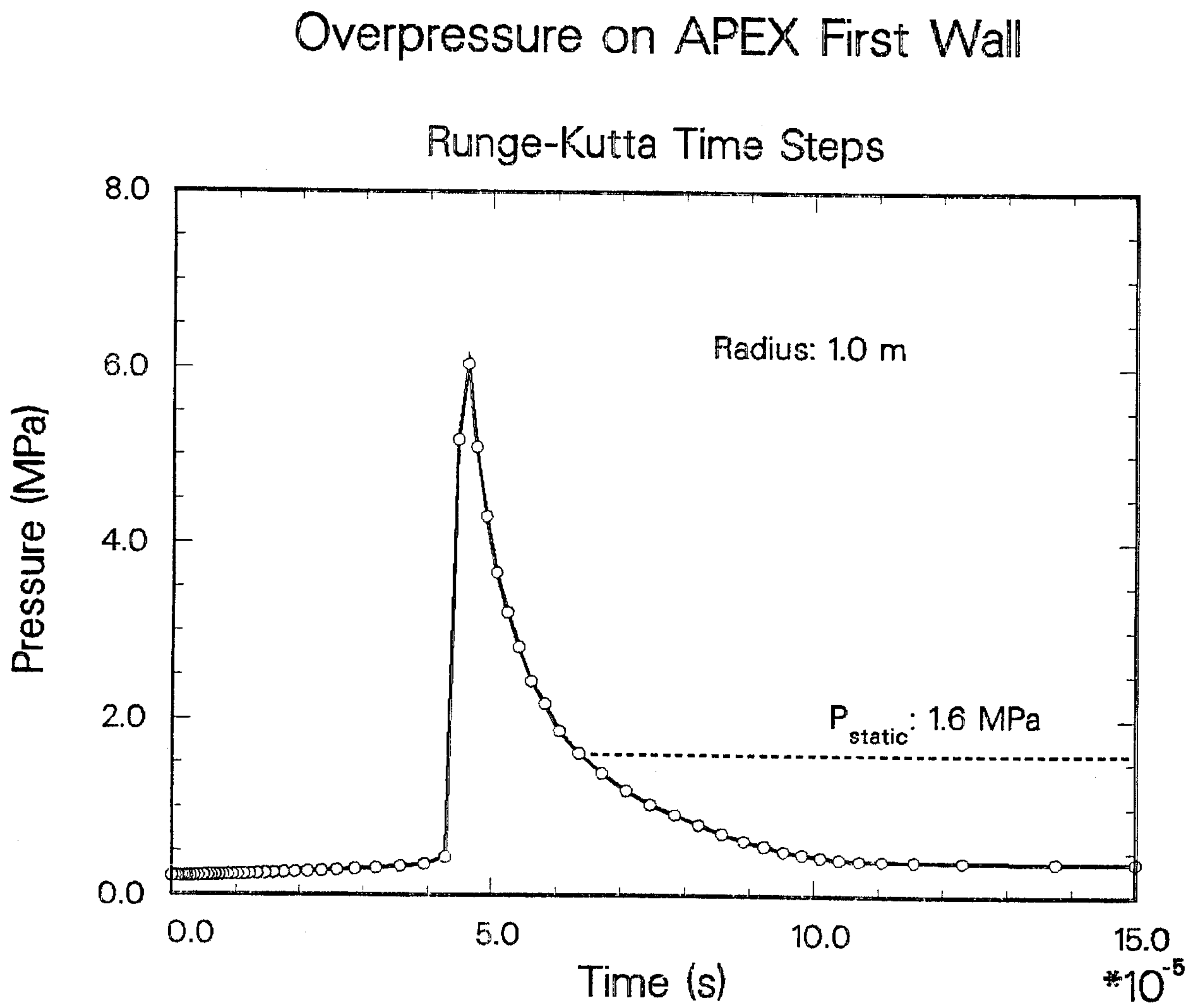

Fig. 7. Pressure on Target Chamber Wall versus Time for APEX. Chamber Radius is 100 cm, Background Gas is 100 Torr Helium.

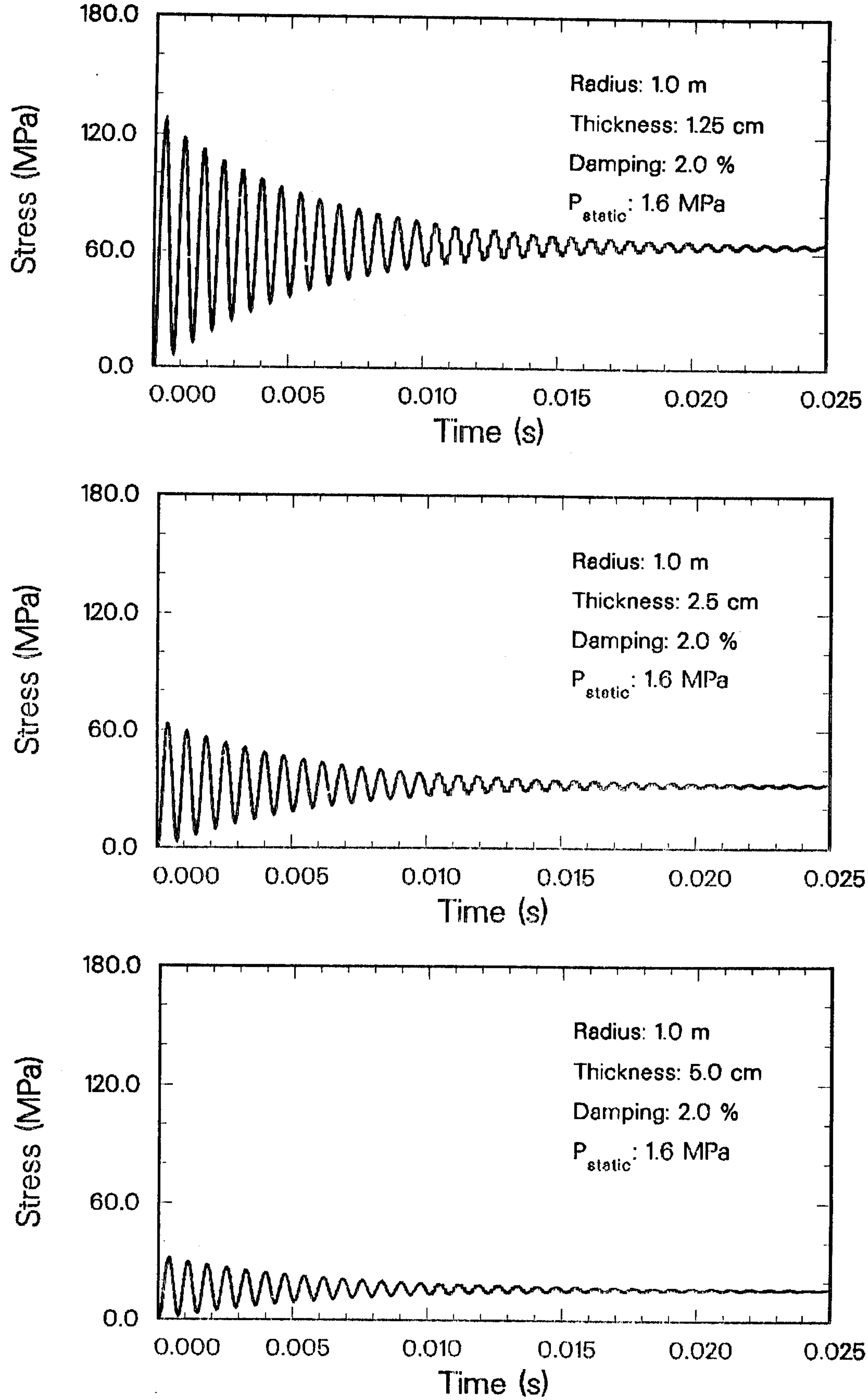

Fig. 8. Mechanical Stress History in Target Chamber for APEX. Chamber radius is 100 cm, background gas is 100 Torr helium. Wall thicknesses are 1.25, 2.5 and 5.0 cm.

where the ions deposit by running a CONRAD simulation with the same vaporized mass as in the high density case but with a low density background. The hydromotion is depicted in the R-T plot in Fig. 9, where one can see that just as with the high density, a shock propagates through the vapor and strikes the wall. The peak pressure from this shock is 14 MPa, which is much larger than the 2.7 MPa peak pressure in the base case. These preliminary results therefore indicate that a low density background gas leads to impulsive wall loadings that may be larger than for a high density background gas.

II.D.3. Wall Without Graphite Liner

We have considered the option of a target chamber first wall which has no graphite liner. The advantage of such a design would be easier construction. The disadvantage would be that the vaporizing material (aluminum or steel) would be much more radioactive than graphite. The disadvantage may be fictitious because vapor from the beam tube and target cryostat and holder will be radioactive in any case. If the vapor mass from the wall is not much greater than that from these other sources the advantages of the graphite liner may be minimal. We expect that the amount of vaporization will be higher without the graphite because of the thermal properties of the materials involved, though the short x-ray stopping lengths in aluminum and steel will definitely play some role. We have not yet done any CONRAD simulations for a bare wall.

II.D.4. Blast Down Beam Tube

The beam transport tube is required for the beam of light ions to reach the target from the diode, a distance of 500 to 600 cm. There are two possible designs of the final focus region of the beam tube: one that is cone

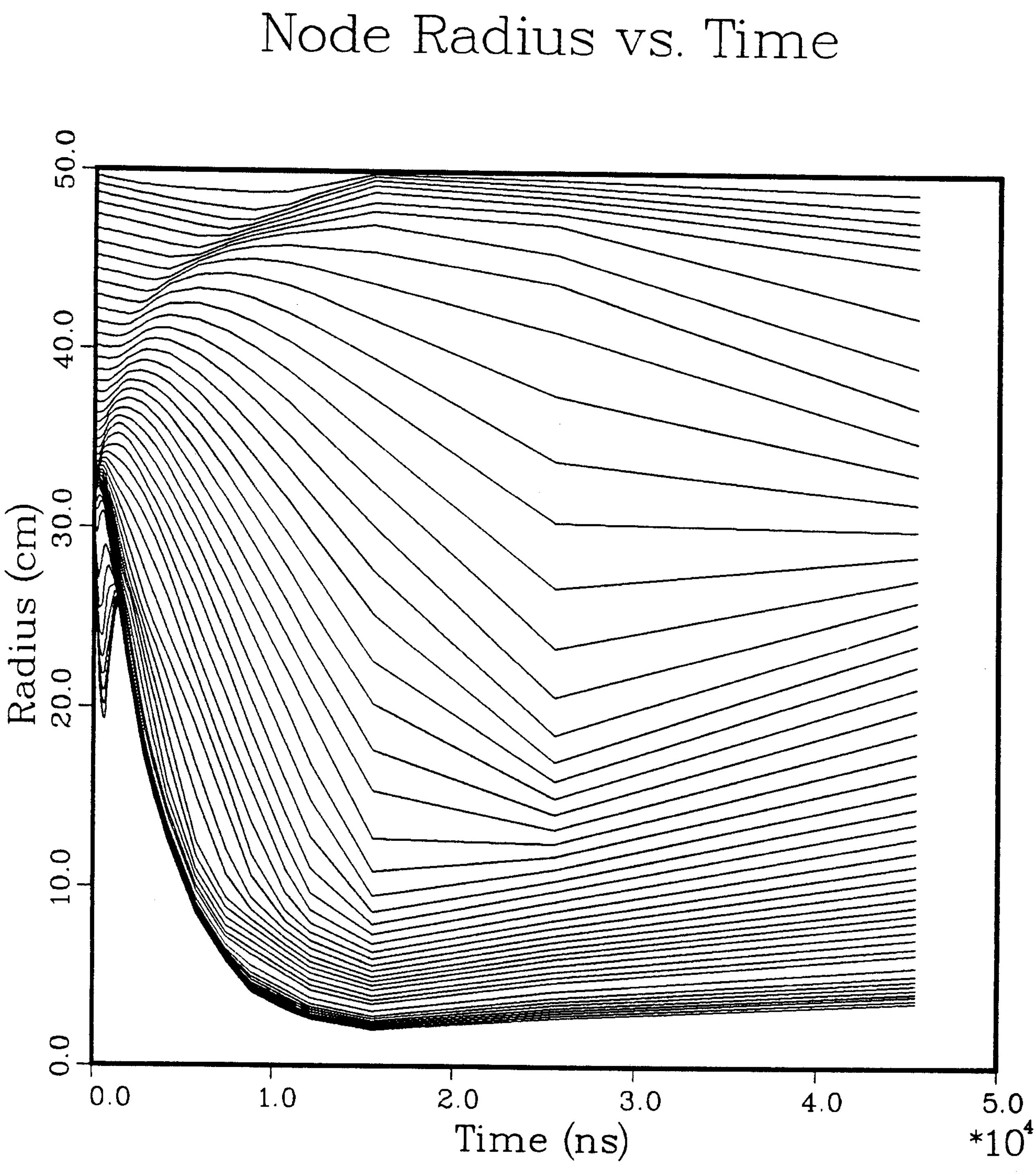

Fig. 9. Positions of Lagrangian Zone Boundaries versus Time for Low Background Gas Density APEX Case.

shaped with the vertex at the target, and one that is just a straight tube. In either case, there must be a fairly high density gas in the focus region and a low density gas in the rest of the beam tube. Throughout most of its length, the beam tube is 2 cm in diameter. This tube may allow a blast wave to reach the diode. We have attempted to simulate the propagation of the blast wave down the beam tube to calculate the mechanical load on the diode.

We have chosen to analyze the conical beam tube only because the other is not very well defined at the present time. The beam tube is shown schematically in Fig. 10. The focus region is filled with 100 torr of nitrogen, while the bulk of the beam tube is filled with 10 torr of hydrogen. The two gases are separated by some type of membrane, which is broken when the ion beam is fired. At the time of beam propagation, we have assumed that the gases in the beam tube are heated to 100 eV.

We begin our CONRAD simulation when the target emanations are depositing in the gases that are in the conditions existing shortly after beam propagation. A first calculation is done in a spherical geometry out to a time when all of the depositions cease. We then simulated the propagation of the blast down the beam tube and found the pressure history on the diode shown in Fig. 11. The maximum pressure on the diode was about 15 MPa.

Much of the hydrodynamic motion down the beam tube may be due to the initial very large pressure gradient that exists between the nitrogen and hydrogen gases. If this is the case, then we would get a large pressure pulse on the diode even if the target does not ignite. The results of a CONRAD simulation with no target explosion are shown in Fig. 12. The maximum pressure on the diode is about 12 MPa.

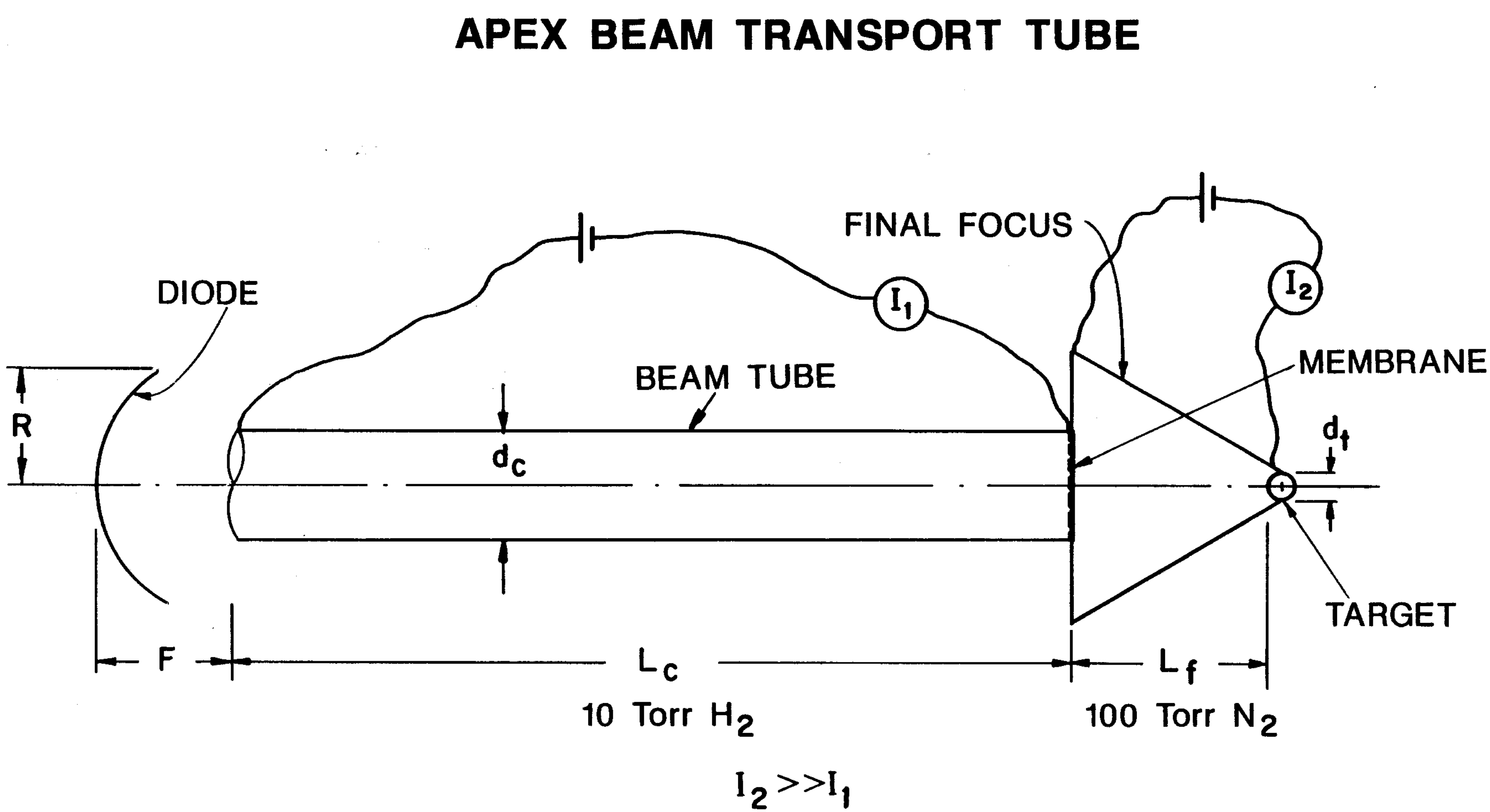

$R = 15$ cm

$F = 150$ cm

$d_c = 2$ cm

$d_t = 1$ cm

$L'_c = 450$ cm

$L_f = 50$ cm

Fig. 10. Schematic Picture of Conical Focus Beam Tube.

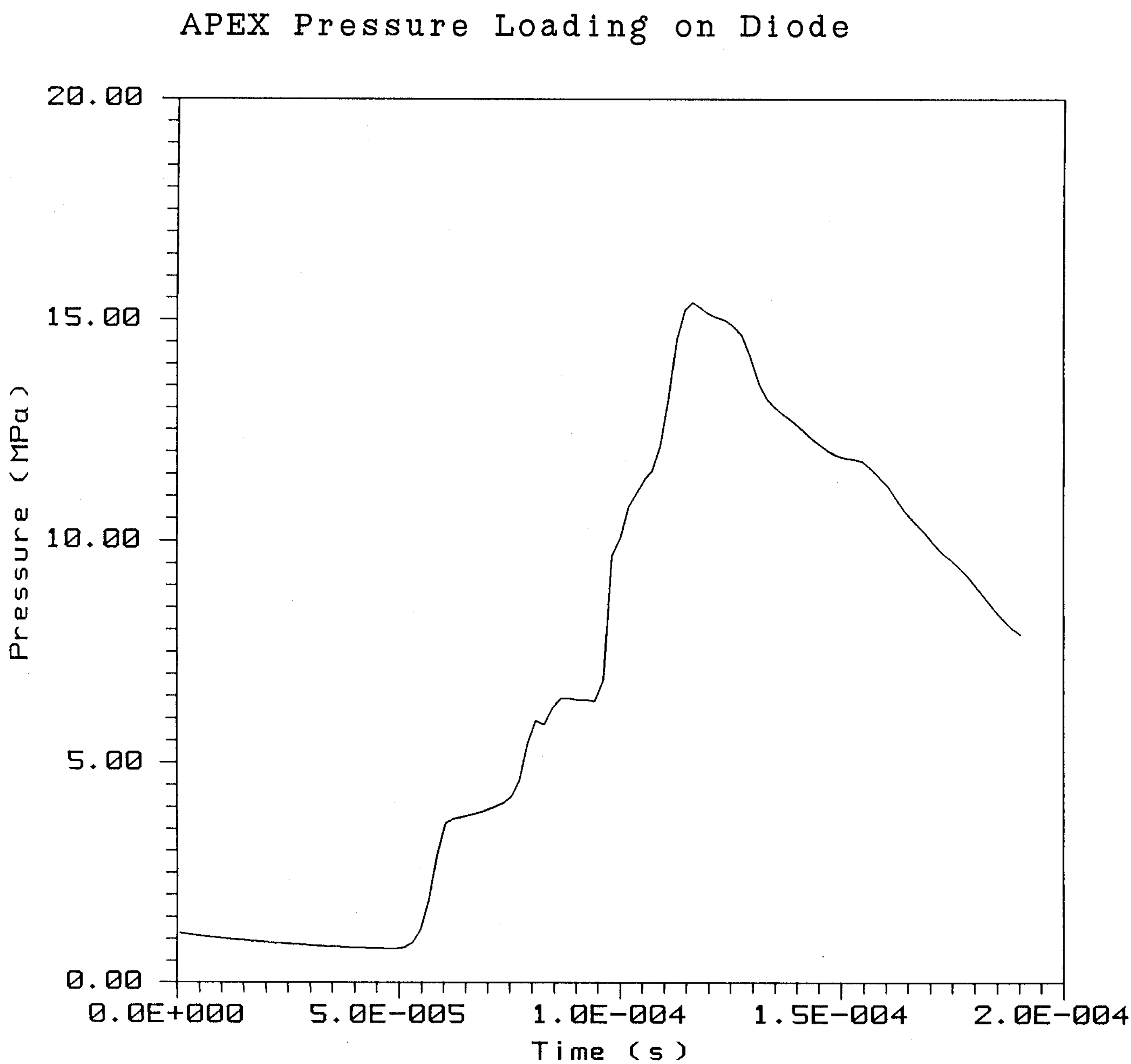

Fig. 11. Pressure History on Diode.

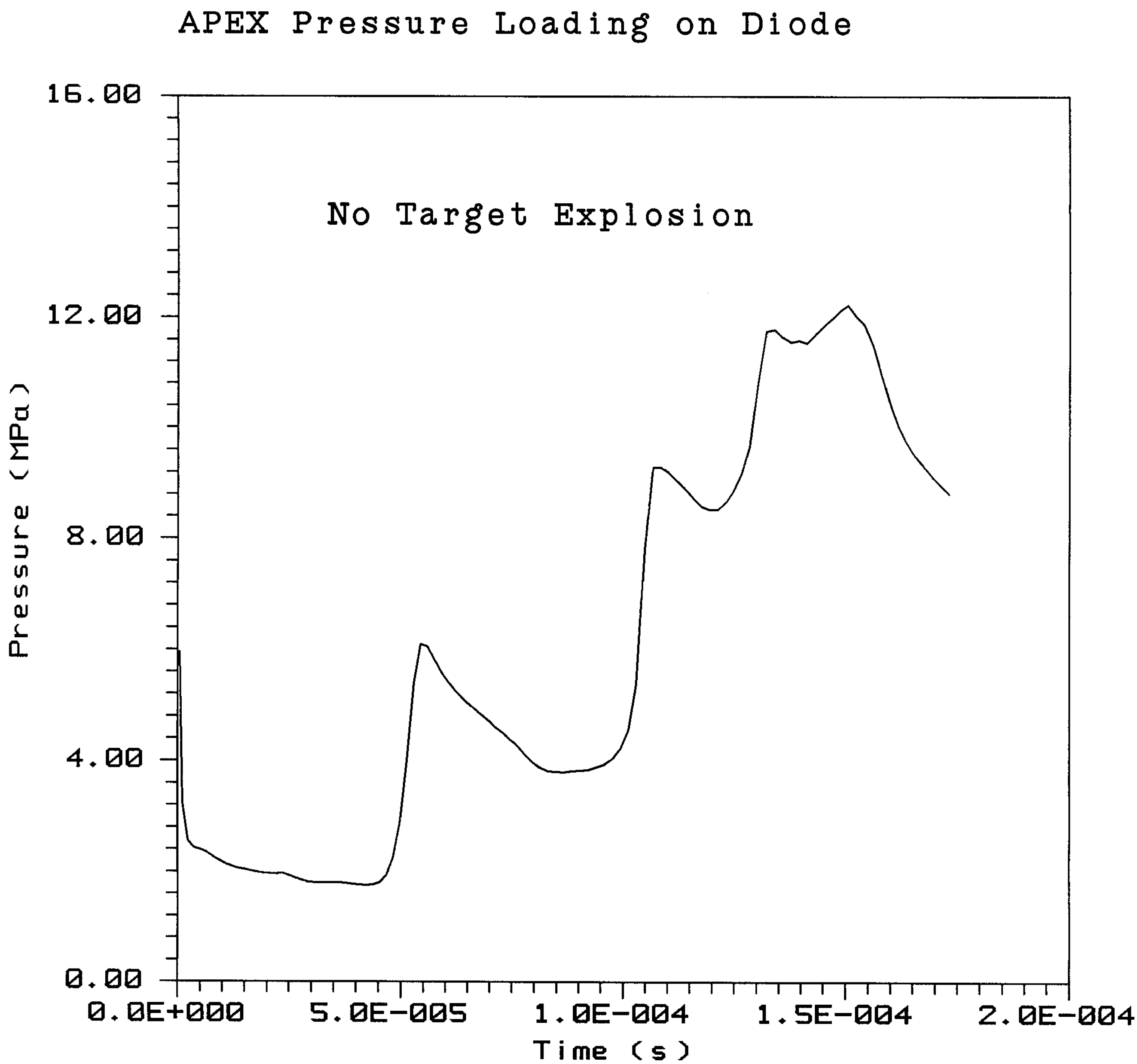

Fig. 12. Pressure History on Diode with no Target Explosion.

We do not know at present what impulse the diode can survive. This depends on the diode design. If the mechanical impulse calculated here is too large, then some additional design is required to protect the diode.

II.D.5. Condensation of Vaporized Materials

The condensation of material that is vaporized by the target blast has been simulated with CONRAD. This is an important issue for the reasons given above and because it influences the gas pressure on the walls of the target chamber. The average gas number density in the fifty centimeter radius base case design is shown in Fig. 13. The target chamber is initially filled with 3.55×10^{18} helium atoms per cubic centimeter. The density shown in Fig. 13 assumes that all of the atoms are carbon, so to have the correct mass density, the effective initial number density is 1.18×10^{18} cm^{-3}. The density quickly rises as roughly 80 grams of graphite are vaporized off of the first wall. The density falls to this initial value at about 0.3 ms after the target explosion.

Vaporized material can be carried throughout the target chamber and the penetrations provided for diagnostics and beam propagation. The vapor is radioactive, so one hopes that the vapor does not travel far from the main part of the target chamber. Simulation of the hydromotion in the target chamber and beam tube show that gas velocities in excess of 10^6 cm/s are present. If 3×10^{-4} s are required for the vapor to recondense, and if the vapor is moving at 10^6 cm/s, then the vapor can travel 3 meters. This means that radioactive material could be carried beyond the shielding if any of the penetrations go through the shielding.

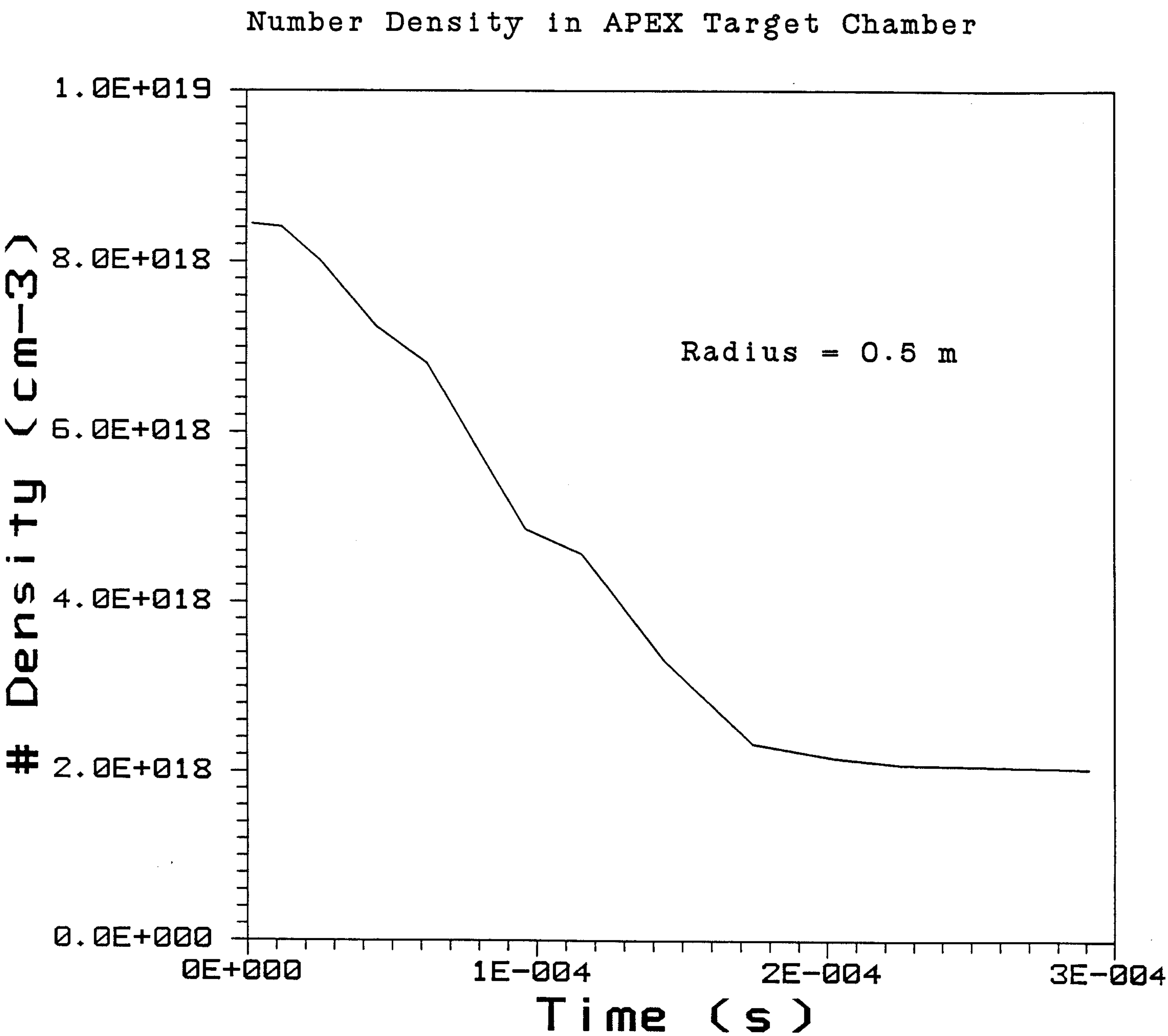

Fig. 13. Number Density in APEX Target Chamber versus Time.

II.E. Conclusions and Recommendations

We have analyzed spherical target chamber designs and believe that a chamber 50 cm in radius with a 5 cm thick wall of aluminum or steel, lined with graphite, will survive at least one 100 MJ target explosion. A target chamber 40 cm in radius may indeed be acceptable, but we have less confidence in any design where the radius is less than 50 cm.

The lack of confidence in smaller cavities results from the complexity of the physical processes present in the target chamber. Vaporization, condensation and blast wave phenomena are all occurring at the same time in the target chamber. We are still testing the computer codes used in obtaining our results. We have done the gas dynamic calculations for the 50 cm radius base case in several ways and have always come to the conclusion that the vessel will survive. We have not done the multitude of calculations required to have the same confidence in the lower radius cases.

We have studied the problem of propagation of the blast wave up the beam tube and believe that there is a danger that the blast wave may destroy the diode. We have found that the pressure pulse on the diode is to a large degree due to the state of the gases in the beam tube after beam propagation and is significant even if there is no target yield. We have not analyzed the mechanical stresses in the diode, but have noticed that the maximum pressure, which is more than 15 MPa, and the mechanical impulse on the diode is larger than that on the wall of the target chamber.

We have several recommendations for areas of further analysis and experimentation to be investigated before the final design of APEX. We are most concerned with resolving the uncertainties in the first wall survival and with the spread of radioactive vapors. Another issue of primary importance is the survival of the ion diode. We also need to further analyze the idea of a bare first wall.

II.E.1. Further Analysis

An essential feature of the target chamber phenomena is the vaporization of material by target x-rays. In this process, x-rays volumetrically heat a region of the wall to energy densities that are high enough to cause very rapid vaporization of as much as a few micro meters of material. The complicated physics of this material partially vaporizing and moving off of the wall determines the recoil impulse on the wall, the amount of radioactive vapor to be condensed, and the protection of the wall from further damage by the target generated blast. Because this process is so important to the viability of APEX, the designers of the facility must be able to predict the amount of vaporization and the speed at which the vapor leaves the wall. We know of no well characterized x-ray vaporization experiments which could verify the accuracy of CONRAD in this regard, so other analyses must be used to do this.

Many of the gas dynamic phenomena are essentially two or three-dimensional in nature. These include the vaporization of the beam tube and target cryostat, blast wave propagation in the target chamber, diagnostic penetrations and beam tube, and condensation of vaporized material. Multi-dimensional simulations need to be done as part of the early design of APEX.

II.E.2. Experiments

The survival of the target chamber should be checked experimentally before APEX is built. We see two parts to the experimentation: verifying that the vessel can survive the anticipated mechanical loading, and verifying that the recoil impulse on the walls due to vaporization agrees with the calculations from CONRAD. The consequences to the rest of APEX and the PBFA-II facility of the failure of the target chamber make this experimentation necessary.

One could test the strength of the target chamber by detonating a chemical explosive in a replica of the target chamber vessel. The amount of explosive used would be that which provides the same mechanical impulse on the vessel walls as a 100 MJ thermonuclear explosion would release. The yield of the chemical explosion would be much less than 100 MJ.

Sandia National Laboratory has the facilities for doing an x-ray vaporization and recoil experiment. One needs a source of x-rays centered around 1 keV and with an intensity of about 600 J/cm^2. One should place a sample of graphite in the path of the x-rays and measure the vaporization and recoil momentum.

ACKNOWLEDGEMENT

This work is supported by TRW through a contract from Sandia National Laboratory. Computer time was partially provided by a grant from the National Science Foundation through the San Diego Supercomputer Center.

III. REFERENCES

II-1. R.R. Peterson, "Gas Condensation Phenomena in Inertial Confinement Fusion Reaction Chambers," University of Wisconsin Fusion Technology Institute Report UWFDM-654 (Oct. 1985) (presented at the 1985 International Symposium on Laser Interaction with Plasma, October 1985, Monterey, CA).

II-2. B. Badger et al., "HIBALL - A Conceptual Heavy Ion Beam Driven Fusion Reactor Study," Kernforschungszentrum Karlsruhe Report KFK-3202 and University of Wisconsin Fusion Technology Institute Report UWFDM-450 (1981) pp V.6-1 to V.6-5.

II-3. R.R. Peterson and T.J. Bartel, "ICF Reactor Target Chamber Issues for the Los Alamos National Laboratory FIRST STEP Reactor Concept," University of Wisconsin Fusion Technology Institute Report UWFDM-580, (1984).

II-4. R.R. Peterson, "Liquid Metal Vaporization and Recondensation and the Repetition Rate of a Liquid Lithium First Surface Inertial Confinement Fusion Reactor," The 1984 IEEE International Conference on Plasma Science, May 1984.

II-5. A.J.C. Ladd, "Condensation of Ablated First-Wall Materials in the CASCADE Inertial Confinement Fusion Reactor," Lawrence Livermore National Laboratory Report UCRL-53697 (Dec. 1985).

II-6. R.O. Bangerter and D. Meeker, "Ion Beam Inertial Fusion Target Designs," Lawrence Livermore National Laboratory Report UCRL-78474 (1976).

II-7. G.A. Moses, G.R. Magelssen, R. Israel, T. Spindler, "PHD-IV, A Plasma Hydrodynamics, Thermonuclear Burn, Radiative Transfer Computer Code," University of Wisconsin Fusion Technology Institute Report UWFDM-194 (revised January 1982).

II-8. G.A. Moses, R.R. Peterson, M.E. Sawan, and W.F. Vogelsang, "High Gain Target Spectra and Energy Partitioning for Ion Beam Fusion Reactor Design Studies," University of Wisconsin Fusion Technology Institute Report UWFDM-396 (Nov. 1980).

II-9. G.A. Moses, "Frequency Dependent X-ray Fluences from a High Yield Light Ion Beam Fusion Target Explosion in a Gas Filled Chamber," University of Wisconsin Fusion Technology Institute Report UWFDM-486 (September 1982).

II-10. R.R. Peterson, "CONRAD - A Combined Hydrodynamics - Vaporization/Condensation Computer Code," University of Wisconsin Fusion Technology Institute Report UWFDM-670 (April 1986).

II-11. T. Mehlhorn, J.M. Peek, E.J. McGuire, J.N. Olsen, and F.C. Young, "Current Status of Calculations and Measurement of Ion Stopping in ICF Plasmas," Sandia Report SAND83-1519 (December 1983).

II-12. R.R. Peterson and G.A. Moses, "MIXERG - An Equation of State and Opacity Computer Code," Computer Physics Communications 28, 405 (1983).